

# Dynamics of Heat Losses from Uninsulated Basement Floors in Houses

R.W. Besant    T. Hamlin    W. Richmond  
ASHRAE Member

## ABSTRACT

In this investigation, the time-varying temperatures of uninsulated basement floors in a few houses were measured and used to compute heat losses. A dynamic model was developed to illustrate the salient features of heat transfer by convection and radiation to the basement floor and its dynamic response.

In this investigation, heat losses through concrete basement floors were examined in 13 houses with well insulated walls and no basement floor insulation. Of particular interest were the modes of heat transfer, the instantaneous, diurnal, and seasonal variations, as well as the total amount of heat lost.

It was found by temperature measurement and air flow measurement that these basement floors lost most of their heat by radiation between the ceiling and the floor. Convection losses were small except when the forced-air circulation system jetted warm air towards the floors, which was usually the case when the furnace came on.

## INTRODUCTION

Heat losses through uninsulated basement floors of houses has played a relatively small role compared to overall space-heat losses. It has been argued that soil temperatures, although perhaps cool are much warmer than ambient air temperatures during the heating season. Thus, heat losses due to air infiltration and conduction through poorly insulated outside windows, walls, and ceilings 1.1 to 22.7<sup>o</sup>F ft<sup>2</sup> hr/BTU (RSI.2 to 4<sup>o</sup>Cm<sup>2</sup>/w), tended to account for about 90 percent of auxiliary space heat requirements.

The advent of super-airtight insulated houses with one-tenth of traditional natural air-infiltration rates, has made the fraction of heat loss through uninsulated basement floors very much larger. These houses typically have extra glazing on windows, RSI 5.3 to 7.0 in walls and RSI 3.5 to 5.3 in basement walls and perhaps RSI 8.8 to 10.6 in ceilings. Although the total amount of heat loss through basement floors may not have changed significantly, up to 50 percent of the auxiliary space heating requirements may be created by losses through the basement floor. Furthermore, the heating requirements for comfortable basements do not match the space heat comfort conditions on the upper floors. This usually leads to uncomfortable basements during most of the year unless special steps are taken to control basement air and floor temperatures.

Traditionally basement floor heat losses were predicted by assuming the ground to be at a fixed temperature with a constant thermal resistance to heatflow from the basement interior to the soil through the basement floor and the adjacent soil [say R-10 (RSI 1.8)].<sup>1,2</sup> Such assumptions are often used to calculate heat losses from uninsulated basement floors during the heating season. During the summer, heat gains through uninsulated or lightly insulated basement ceilings and walls tend to keep basement air temperatures near the comfort zone so that no additional heat is required in most basements of standard construction.

---

ROBERT W. BESANT	DEPT. OF MECHANICAL ENGINEERING
TOM HAMLIN	UNIVERSITY OF SASKATCHEWAN
WILLIAM RICHMOND	SASKATOON, SASKATCHEWAN

In new low energy houses, the traditional approach to basement floor heat-loss calculations can lead to serious errors. Measurements indicate that basement floor temperatures are not uniform over the floor nor are they constant in time. The floor temperatures partly depend on the proximity and thermal contact with exterior concrete walls and adjacent soil. The soil temperatures vary seasonally, with the south-facing soil temperatures showing a solar gain effect in the spring. Most importantly, basement floor surface temperatures depend on air circulation rates and air and ceiling temperatures in basements. That is, when a house calls for auxiliary space heat as controlled by a thermostat on the upper floor during the heating season, jets of warm air are usually directed at the basement floor. This not only warms the basement floor slightly in the region of the air jets; it increases the heat losses from the entire basement floor during that period because of increased air mixing and radiation from the ceiling. It is noted that because of the relatively huge thermal capacitance of the basement floor and the soil underneath it compared with that of the basement air (approximately 500:1), the changes in floor surface temperatures remain small unless heat is added over a very long period of time. Furthermore, with uncomfortably cool soil temperatures all year round, uninsulated basement floor temperatures do not reach a condition of comfort and zero heat loss under normal operating conditions. Finally, with the high levels of wall insulation and low air circulation rates in low-energy houses during spring, summer, and fall, heat gains to the basement air are often insufficient to maintain comfort conditions in such periods.

Because these dynamic thermal phenomena associated with uninsulated basement floors in low-energy houses are very significant, a new method of analysis of basement floor heat losses is proposed. This method utilizes temperature data on the surfaces of basement floors, walls, and ceilings as well as air temperatures and air circulation rates.

The advantage of this method is that it presents a much more accurate time-dependent model of the consumption of auxiliary space heat by the basement floor. The heat loss rates can be made to match the actual energy used as a function of time. The main disadvantage of such a method is that more data is required for basement temperatures and airflows.

In this paper, the basements of several low-energy houses have been examined for the net heat transfer rates to the basement floors by radiation and convection heat transfer during 1981 and 1982. The thermal design details of these basements is presented in Tab. 1.

#### TEMPERATURE AND AIR FLOW DISTRIBUTION IN THE LOW ENERGY HOUSES' BASEMENTS

In order to gain a more complete understanding of basement floor heat losses, it is necessary to measure the temperature distributions on all interior surfaces as well as the air temperature profiles near the floors in question. Furthermore, air velocities in the vicinity of the floors are necessary to estimate heat transfer coefficients to the floor.

The temperature of the various surfaces and the air were measured using a calibrated resistance temperature sensor, given an absolute error in readings of less than  $.5^{\circ}\text{F}$  ( $0.3^{\circ}\text{C}$ ). The difference in temperature measurements is probably accurate to  $.2^{\circ}\text{F}$  ( $0.1^{\circ}\text{C}$ ). A thermally conductive grease was used to ensure a good contact with the various surfaces. Readings were recorded after the indicator reached thermal equilibrium which usually meant a 30- to 60-second time delay.

Air speeds were measured using a calibrated hot-wire anemometer air-speed indicator which could read air speeds as low as  $.16$  ft/sec. ( $0.05$  m/sec.). Air movement below this speed was sensed by a tufted wool probe.

Some results of the temperature measurements on some different basement floors are presented in Figs. 1 to 3. These results indicate a considerable variation in temperature on the basement floors, especially for split level designs. It is also noted that the basement mid-height air temperature differed from house to house. The variation in air temperatures with height from a basement floor for one house is indicated in Figs. 4 and 5. These figures show that the variation in air temperature with height is dependent on the fan speed and, more importantly, furnace auxiliary heating. With the furnace running continuously for more than one-half hour, the floor temperature rises especially in the area under the air circulation jets. It appears that the buoyant effects of the warm air tend to stratify the air temperature much more with the added warm-air jets on than when there is no air circulation.

Airflows and temperatures from basement heating air ducts were measured in only one house, M1. In this house, hot air exhausted from the air duct down from the ceiling farthest from

the furnace reached a steady temperature of 97°F (36°C) about 15 minutes after the furnace was turned on. The average temperature in this duct for a 20-minute furnace on time would be about 93°F (34°C). Duct outlet temperatures for other houses ranged between 86 and 122°F (30 and 50°C). The air speed in the duct remained nearly steady during the whole furnace on time at an average value of 3.28 ft/s (1.0 m/s).

#### ANALYSIS OF THE MEASURED DATA AND RESULTS USING QUASI-STEADY CONDITIONS

Heat transfer to concrete basement floors takes place by means of radiation from the surrounding surfaces and convection from the adjacent air movement. The complexity of the physical situation as implied by the temperature distribution data and time-dependent airflows suggests that some degree of simplification of the data for purposes of analysis is desirable. One such simplification is to use a mean effective basement floor temperature for radiation and another one for convection. For radiation, this temperature was calculated from the equation:

$$T_R^4 = \frac{1}{A} \sum T_i^4 A_i \quad (1)$$

and for convection the mean floor temperature is:

$$T_C = \frac{1}{A} \sum T_i A_i \quad (2)$$

where

A is the total floor area, and

A<sub>i</sub> is the area of floor area element whose temperature is T<sub>i</sub>.

The results of using the 1981 spring data in these equations for all the houses showed that

1.  $T_R \approx T_C = \bar{T}$

2. the concrete floor temperature distribution was such that they would have a value of  $\bar{T}$  3.94 to 4.92 ft. (1.2 to 1.5 m) distance from any outside wall provided it were not near a corner, underground plumbing, gas pipeline, wiring ducts, basement floor insulating covers such as boxes or thick rugs, or exhausts from air heating ducts.

In the future it may be possible to use a single temperature measurement to establish an accurate floor temperature. More research work is suggested to verify such an assumption.

The basement floors in each house that was tested not only had a slightly different physical design configuration but also had a significantly different operating configuration. Some floors were completely bare, others had carpet, others were covered in packing boxes, etc. These features change the heat-loss characteristics of these floors.

Operating configurations were estimated by observation of each basement. The results are presented in Tab. 1. All of the houses had hot-air distribution systems except one, C1. The number of active air-heat ducts in the basements were noted for each house and are shown in Tab. 4. It is further noted that some of the house designs called for continuous air circulation regardless of whether space heat was required or not. No measurements were taken to indicate when the air circulation fans were on in each house; however, the time duration of furnace on time can be inferred directly from the measured space heat fuel consumed as given in Tab. 2.<sup>3</sup> The large discrepancy between measured and predicted space-heat consumption in this table is accounted for in part by using traditional basement floor heat losses of 2.5 Btu/hr ft<sup>2</sup> (8 w/m<sup>2</sup>). In most houses, the furnace would have been on about 25% of the time during an average heating season from October 1 to April 30.

The calculation of radiation heat transfer to basement floors was accomplished assuming that the ceiling and floor were at uniform temperatures and that the well insulated basement walls were adiabatic. The radiation shape factors from the ceiling to floors and walls were included in the calculation. The surface emissivities were taken to be .9 for all surfaces. It was assumed that the covered portion of each floor did not participate in the heat radiation process, but that the carpeted area did. The computed results for the 14 houses are given in Tab. 3.

The calculation for the convective heat transfer to the floors is more complex than that for radiation because there are several modes of airflow in each of these basements. These

different modes of convective heat transfer are (1) natural convection with no forced air circulation, (2) forced convection with the air-circulation fan on, but with no furnace heat, and (3) forced convection with the furnace and the air circulation fan on. When the furnace fan is on air is rapidly circulated from the ducts down to the floor in those regions of the floor directly exposed. When the furnace is also on, the temperature of this circulated air is much warmer than room air so the heat rate to the floor in the region of the ducts is quite high.

Details of the convective heat transfer calculations are presented in Appx A. The results of these calculations for the 14 houses are presented in Tab. 3. Included in these results are the assumptions that the floors are partially covered in carpet and partially in boxes and material with a high insulation effect as given in Tab. 1. The thermal resistance of the carpets were taken to be  $2.27 \text{ }^\circ\text{F ft}^2 \text{ hr/Btu}$  ( $0.4 \text{ }^\circ\text{Cm/w}$ ).

The estimated average total heat loss rate to the basement floors in eight houses were calculated for different times of the year and different average modes of operation. (See App. C).

#### THE DYNAMICS OF BASEMENT FLOOR TEMPERATURES

Measurements of basement floor temperatures revealed significant changes from day to day and month to month. Figure 6 presents data on variations in floor temperatures over the seasons. These data show two general trends, namely, ones that follow ambient soil temperature variations and those that showed a rapid increase in temperature with the onset of the heating season. It is speculated that the heating season induced increased heat transfer from the furnace to the basement floor in the latter case. However, heat loss rates to the basement floors in the former case were somewhat constant because of constant air circulation and electrical and solar gains during summer as shown in Tab. 4.

The measured floor temperatures as presented in Fig. 6 were extrapolated for each month of the year using soil temperature data. These estimated floor temperatures were then used to compute the basement floor heat losses using the calculation method presented in Eqs. 1 and 2. The results of these and other calculations are presented in Tab. 3 and 5.

More extensive data is presented for house A1 in which strategically placed thermocouples were monitored continuously every 15 minutes through the heating season. These data are presented in daily-averaged form in Fig. 7. Figure 8 presents the 15-minute time average data. In these figures, the relationship between furnace operation and basement floor temperature reflects the heat loss phenomena.

A lumped parameter dynamic model was developed, as presented in Appx B, to interpret this time-varying temperature. Using the ceiling, floor, and air temperature averages, the magnitude of heat loss to the floor was calculated at each instant. In the model, the first node at the floor was assumed to have the capacitance of the concrete floor associated with it. From the plots of energy flows and temperatures, basement heat loss can be seen to be a very dynamic phenomena highly influenced by activity in the basement. The relatively large thermal capacitance of the soil along with its slow thermal resistance cause the floor to remain at low temperatures.

#### DISCUSSION AND CONCLUSIONS

It can be seen from the results calculated in Tab. 3 that basement floor heat loss rates vary considerably. These variations depend on

1. the design of the basement floor and its surrounding soil, walls, etc.
2. the configuration of floor covering
3. the furnace and air circulation fan operation in the basement

Furthermore, the results suggest that basement floor heat losses in low-energy houses may be twice as great as what traditional methods of calculation would suggest. As a consequence of these high heat loss rates from basement floors, a calculation of the total heat rate from low-energy houses using traditional methods could differ substantially from measured results. This suggests that the basement floor of each house must be considered separately using detailed heat transfer calculations.

The data in Tab. 3 was based on standard ASHRAE methods of calculating heat losses except for the basement floor which was calculated using measured and interpolated data on floor and ceiling temperatures, furnace and fan on times, floor covering and summer solar gains and air circulation. This method of basement floor heat loss calculation is outlined in App. C. It is noted that directed methods of measuring basement floor heat losses such as mimic boxes do not account for radiation transfers which are usually more important than convective heat transfer. Heat flux meters with internal thermal conductivities significantly different than concrete floors may alter the local heat flow characteristics significantly in the vicinity of the heat flux meter with the result that large errors may result. As a consequence of these inherent problems it was concluded that the proposed method of calculating basement floor heat fluxes would be at least as accurate, and had the advantage of being able to represent the dynamics of these heat fluxes.

It is noted that these results are considered preliminary because there was a very limited amount of data available from a few houses. Errors in these results could result from many sources, especially in the sampling of data that was necessary in this study. Also, better heat-transfer correlations for basement floors could change the quantities calculated significantly.

The dynamics of basement floor temperatures suggests a strong coupling of furnace heat inputs to the basement floor and the floor temperature. The simplified model presented in this paper illustrates the observed behavior in one typical house. Much more data would be required to validate and quantify the model parameters for a large class of houses.

#### APPENDIX A CONVECTION HEAT RATES TO BASEMENT FLOORS

The method of calculation of convective heat transfer to basement floors is presented in this appendix. In this method, there are two distinct modes of convective heat transfer to basement floors, natural convection and forced convection as supplied by the furnace fan.

For natural convection, the method of calculating the heat rate is<sup>5</sup>

$$Q = h A (T_1 - T_a) \quad (A.1)$$

where

A is the floor area

$T_1$  is the average floor temperature

$T_a$  is the room air temperature at a height of 0.8 m, and

h is the convective heat transfer coefficient as given by the correlation<sup>6</sup>

$$h = Nu(k/L) \quad (A.2)$$

$$Nu = \sqrt{f} \frac{(1 - 2.2 \sqrt{f})}{1 + 0.2 (H/d - 6)} \sqrt{f} \left[ 1 + \left( \frac{H/d}{6/f} \right)^{6 - .05} \right] Re^{2/3} Pr^{.42} \quad (A.3)$$

over the entire floor area,

where

f is the relative nozzle area, and

H is the distance from ceiling to floor.

Typical results for this correlation for  $f = .001$ ,  $Re = 9000$ ,  $H/d = 20$  gives for the bare and carpeted floor area

$$h = 2.0 \text{ w/m}^2 \text{ } ^\circ\text{C} \quad (A.4)$$

In the final calculations used in Table 3, the value of h was taken to be  $2 \text{ w/m}^2 \text{ } ^\circ\text{C}$ . This is approximately the value that can be inferred from the data presented in Fig. 5, which shows the rise in floor temperature as a result of turning on the furnace for a 30-minute period. It is also clear from this figure that the heat radiation rate will increase insignificantly as a result of running the furnace. Theoretically, the heat radiation rates in Tab. 3 should also be increased to more accurately model the heat loss rates to the basement floor. This may suggest that the effective average convective heat rates (including radiation) should be higher than  $2.0 \text{ w/m}^2 \text{ } ^\circ\text{C}$  when the furnace is on. Finally, it is noted that although the average value of heat transfer coefficient is taken to be  $2 \text{ w/m}^2 \text{ } ^\circ\text{C}$ , it is by no means constant over the entire floor. More research is required to obtain better data for h.

APPENDIX B  
DESCRIPTION OF DYNAMIC BASEMENT FLOOR LUMPED PARAMETER MODEL

The model used to simulate the dynamics of a basement floor is shown below. It consists of two thermal masses--the concrete floor and a soil lump beneath the floor. Heat transfer to or from the basement floor occurs as the result of radiation from the ceiling above the floor and convection from the air in the basement. Each thermal mass is assumed to have negligible thermal resistance within itself. However, an arbitrary conductive resistance is put between the floor and the soil beneath the basement. The soil lump is of a finite volume beneath the basement floor, and it loses heat through the soil to the surface and to the soil beneath it. Because the basement walls of a typical energy-conserving home would be insulated, it has been assumed that the walls are adiabatic. Heat loss from the floor is assumed to occur only to the soil lump.

$T_C$ = ceiling temperature	$R_{12}$ = thermal resistance between floor and soil lump
$T_a$ = air temperature	$T_2$ = soil lump temperature
$T_1^a$ = floor temperature	$M_2$ = mass of soil lump
$M_1^l$ = mass of floor	$C_{P2}$ = specific heat of soil lump
$C_{P1}$ = specific heat of floor	$R_{a1}$ = thermal resistance between air and floor
$R_{C1}$ = thermal resistance between ceiling and floor	$R_{G2}$ = thermal resistance between soil lump and soil beneath soil lump
$R_{S2}$ = thermal resistance between soil lump and surface	$T_G$ = temperature of soil beneath soil lump
$T_S$ = soil surface temperature	

As shown in the model, the ceiling, air, surface, and soil beneath the soil lump are shown as time-dependent variables. These, however, are known values. A data-acquisition system permitted the measurement of actual ceiling and air temperatures at frequent time intervals, and data collected by the Saskatchewan Research Council gave daily and average monthly soil temperatures for Saskatoon.

The differential equations describing the simplified model appear below in Eq. A.1 and A.2.

$$M_1 C_{P1} \left( \frac{dT_1}{dt} \right) = \frac{T_a - T_1}{R_a} + \frac{T_e - T_1}{R_c} + \frac{T_2 - T_1}{R_{12}}$$

$$M_2 C_{P2} \left( \frac{dT_2}{dt} \right) = \frac{T_1 - T_2}{R_{12}} + \frac{T_s - T_2}{R_{S2}} + \frac{T_G - T_2}{R_{G2}}$$

The resistances are simply:

$$R_a = \frac{1}{h_a A}$$

where

$h_a$  = convective heat transfer coefficient of the air  
 $A$  = floor area

$$R_c = \frac{\frac{2(1-\epsilon)}{\epsilon} + \frac{2(1-\epsilon)/\epsilon + (2 F_{1C}/F_{1-W})/(1 - F_{1C}/F_{1-W})}{A \sigma (T_C^2 + T_1^2) (T_C + T_1)}}$$

where

$\epsilon$  = emissivity  
 $F_{1C}$  = shape factor from floor to ceiling  
 $F_{1-W}$  = shape factor from floor to basement walls

$$\sigma = 5.6696 \times 10^{-8} \text{ w/m}^2 \text{ K}^4$$

$$R_{12} = \frac{L_{12}}{K_{12}A}$$

where

$L_{12}$  is the assumed depth of soil between masses 1 and 2  
 $K_{12}$  = thermal conductivity of soil

$$R_{S2} = \frac{1}{K_{S2}S_{S2}}$$

where

$K_{S2}$  = thermal conductivity of soil  
 $S_{S2}$  = shape factor between soil lump and surface

$$R_{G2} = \frac{1}{K_{G2}S_{G2}}$$

where

$K_{G2}$  = thermal conductivity of the soil  
 $S_{G2}$  = shape factor between soil lump and soil lump and soil beneath the soil lump

#### METHOD OF SOLUTION OF DIFFERENTIAL EQUATIONS

Equations B1 and B2 were solved simultaneously using a Runge Kutta-Verner fifth and sixth order method for solving differential equations. The Runge Kutta-Verner subroutine used in the computer model was the IMSL Library subroutine DVERK.

#### COMPUTER MODEL

##### Description

The computer program utilizes data that was collected on a data acquisition system at 15-minute intervals. It includes the ceiling, air, and basement floor temperatures and the average rate of energy consumption of the gas furnace. The program, with the input of the various resistances, the specific heat of the two masses, soil temperatures ( $T_S$  and  $T_G$ ), other necessary parameters, and an initial guess at the temperatures of the two thermal masses, then recalculates the temperatures of the floor and the soil lump at 15-minute intervals.

Before the subroutine to solve the differential equations is called, the calculations seen immediately before the call are performed. Since the program calculates the temperatures of the floor and the soil over a 15-minute interval, ceiling and air temperatures were averaged over the time from (I-1) to I. Because the heating system for the house that was analyzed was a forced-hot-air gas furnace, both the temperature of the air above the floor and the convection heat transfer coefficient will vary with the operation of the furnace. Using the factor F, which gave the fraction of the time interval the furnace was actually operating, formulas were written to give a convection heat transfer coefficient and an air temperature that would reflect the operation of the furnace.

The model was validated against an analytical two-lump solution.

#### APPENDIX C BASEMENT FLOOR HEAT FLUX CALCULATIONS

The heat flux to the basement floors were calculated assuming that the flux was provided by convective heat transfer from the ambient basement air plus the net radiation heat transfer using the following linearized equation

$$Q = h_e A_c (T_a - T_1) + h_r A_r (T_2 - T_1)$$

where

$A_c$  = the uncovered or carpeted floor area  
 $h_c$  =  $(1/h_c + r_c)^{-1}$  the equivalent convective coefficient  
 $h_e$  = the convective heat transfer coefficient ( $2 \text{ W/m}^2 \text{ } ^\circ\text{C}$ )  
 $r_c$  = the specific carpet thermal resistance ( $.4 \text{ m}^2 \text{ } ^\circ\text{C/W}$ )  
 $T_a$  = the average air temperature at 0.8m height or when the furnace was on,  
 $T_e$  = the average air duct exhaust temperature  
 $T_f$  = the average concrete floor temperature  
 $A_f$  = the uncovered floor area  
 $T_r$  = the average ceiling temperature (about  $21^\circ\text{C}$ )  
 $h_r$  = the linearized radiation coefficient

$$= \frac{(T_f^2 + T_r^2) (T_f + T_r)}{(1 - \epsilon_1)/\epsilon_1 + 1/(F_{12} + [1/F_{1R} + A_1/A_2 F_{2R}]^{-1}) + A_1 (1 - \epsilon_2)/A_2 \epsilon_2}$$

$\sigma$  = the Stefan Boltzmann constant  
 $\epsilon_1$  = the emissivity of the floor (.9)  
 $\epsilon_2$  = the emissivity of the ceiling (.9)  
 $F_{12}$  = the shape factor from floor to ceiling  
 $F_{1R}$  = the shape factor from floor to walls  
 $F_{2R}$  = the shape factor from ceiling to walls  
 $A_1$  = the uncovered floor area  
 $A_2$  = the ceiling area

The radiation heat transfer coefficient  $h_r$ , was based on a model of gray body radiation heat transfer from the ceiling to the floor with an adiabatic participating surface, namely the outside walls. Calculation of the average wall surface temperature for zero net radiation transfer to the outside walls showed that the average measured wall temperatures were within one degree Celcius of the predicted value for the case of well insulated walls. Thus for basement floor heat fluxes the net radiation exchange to the outside walls is negligible.

In the calculation of heat fluxes to the basement floors the furnace activation time was estimated using the fuel consumption data and the measured furnace burn rate. Calculations of basement floor heat fluxes were calculated for the average surface temperatures and furnace operating time each month. These conditions were adjusted for each month of the year.

#### REFERENCES

1. J.K. Latta and G.G. Boileau, "Heat Losses From House Basements", NRC, DBR, Housing Note 31, Oct. 1969.
2. ASHRAE Handbook of Fundamentals (1977).
3. R.W. Besant, "The Thermal Performance of 14 Low Energy Homes in Saskatoon, Saskatchewan, January 1 to April 2, 1981", Report, Dept. of Mechanical Engineering, June 1981.
4. R.W. Besant and T. Hamlin, "The Measured Performance of Low Energy Passive Solar Houses for 1981-1982", Report, Dept. of Mechanical Engineering, August 1982.
5. B.V. Karlekar and R.M. Desmond, Engineering Heat Transfer (West Pub. Co., 1977).
6. H. Martin, "Heat and Mass Transfer Between Impinging Gas Jets and Solid Surfaces", Advances in Heat Transfer Vol. 13 (Academic Press, 1977).



TABLE 1

Design and Operating Configurations for 14 Low Energy Houses in Saskatoon, Saskatchewan

House	Base Type	Floor Design			Wall Design Above Ground			Wall Design Below Ground			Estimated Floor Configuration	
		Type	Area	Added RSI	Type	Height (m)	Area (m <sup>2</sup> )	RSI °C m <sup>2</sup> /w	Height (m)	Area (m <sup>2</sup> )		RSI °C m <sup>2</sup> /w
M1	FULL	CONC	98.40	0	CONC	.5	21.94	7.0	1.8	77.11	5.0	90%B 10%C 40%B 60%C 20%B 70%CC 10%C
E1	FULL	CONC	98.90	0	CONC	.3	20.80	4.5	2.0	91.19	3.5	
S1	FULL	CONC	102.34	0	FRAME	1.3	50.42	9.5	1.0	42.12	3.9	
C1	FULL	FRAME	64.20	0	FRAME	1.3	40.69	7.0	1.0	41.50	7.0	90%CC 10%C
C2	FULL	CONC	88.61	0	CONC	.2	18.77	5.3	2.0	91.70	5.3	20%B 70%CC 10%C
A1	FULL	CONC	95.66	0	CONC	.3	21.65	4.9	2.0	89.20	3.9	100%B
V1	FULL	CONC	96.33	0	CONC	.4	22.5	3.9	2.0	87.2	3.9	10%B 70%CC 20%C 70%B 30%CC 90%B 10%C
P1	UPPER	CONC	27.4	0	FRAME	1.3	21.84	5.6	1.1	18.48	3.8	
	LOWER	CONC	68.3	0	CONC	.2	11.4	5.6	2.1	59.85	3.8	
C3	UPPER	CONC	28.8	0	FRAME	2.4	13.2	4.8	0	0	3.9	90%CC 10%C
	LOWER	CONC	54	0	CONC	.9	18.9	4.8	1.5	31.5	3.9	80%B 20%C
S2	UPPER	FRAME	41.2	NA	FRAME	1.1	12.32	6.0	1.3	14.56	2.1	20%C 80%CC
	LOWER	CONC	41.2	0	CONC	.5	5.6	3.5	1.8	20.16	2.1	50%CC 20%B 30%C
C4	UPPER	FRAME	66	0	FRAME	.8	28.26	4.8	1.5	32.6	4.8	10%B 70%CC 20%C
	LOWER	FRAME	39.36	0	FRAME	.3	5.34	4.8	2.1	37.38	4.8	
N1	UPPER	CONC	50.4	0	CONC	1.4	27.02	7.0	1.0	19.3	4.9	
	LOWER	CONC	43.1	0	CONC	.3	7.77	4.9	2	51.8	4.9	50%CC 40%B 10%C
S3	FULL	CONC	106.00	0	FRAME	1.5	50.34	4.9	.9	41.95	3.5	40%B 50%CC 10%C
M2	FULL	CONC	101.00	0	CONC	.4	15.64	5.6	1.9	87.0	5.6	10%B 20%C 70%CC

## NOTES:

B - bare  
C - covered  
CC - carpeted

TABLE 2

Energy Consumption and Calculated Performance of 14 Commercially Designed  
And Contracted Low Energy Houses In Saskatoon (lat 52° 6')  
March 5, 1981 to March 2, 1982

House Code	Heated Floor Area m <sup>2</sup>	Induced Air Change at 50 pa ACH-1	Measured Consumption			Performance Space Heating Energy Consumption	
			Nat. Gas m <sup>3</sup>	Elect. kw-hr	Water m <sup>3</sup>	Measured <sub>2</sub> KJ/(DD-m <sup>2</sup> )	Predicted <sub>3</sub> <sup>+</sup> KJ/(DD-m <sup>2</sup> )
M1	198.4	.53	694	12940	---	---	21.1
E1	200.5	.37	1656	13196	427	24.9	7.0
S1	204.6	1.09	1883	15651	549	28.6	12.8
P1	228.0	.76	2364	11357	598	41.9	12.5
C1	128.4	2.19	2818	7000*	342	85.4	40.0
C2	194.7	.77	2316	10131	485	50.6	18.3
A1	205.0	.62	1665	9623	491	42.3	16.7
V1	197.0	.45	2800	8741	397	71.9	34.0
C3	199.0	1.04	---	---	---	---	14.3
S2	164.8	1.14	2627	8674	353	81.4	22.2
C4	209.4	1.31	2607	8230	239	69.6	30.8
N1	196.4	.76	2161	6142	242	58.8	37.3
S3	212.0	.54	3106	10037	404	68.6	28.0
M2	202.5	.74	2401	8084	425*	44.5	22.7
Ave.	195.8	.88					
Std. Dev.	14.5	.45					

## NOTES:

1. Natural gas heating value taken as 38.16 MJ m<sup>-3</sup> one fifth of water used assumed DHW requiring 283 MJ m<sup>-3</sup> (3031 Kwhr of space heat assumed in house M1).
2. Saskatoon received 5734 DD relative to 18°C base (-10,500 DD relative to 65°F base) for the measurement period.

\* estimated

+ predesign predicted using total heated floor area

TABLE 3

Annual Modified Design Analysis Results of Heat Loss Components for 14 Low Energy Passive Solar Houses In Saskatoon, Saskatchewan.

House	Ceiling		Walls		Doors		Basement Walls Above Ground		Basement Walls Below Ground		Basement Floor		Windows		Infiltration	
	GJ	Ratio	GJ	Ratio	GJ	Ratio	GJ	Ratio	GJ	Ratio	GJ	Ratio	GJ	Ratio	GJ	Ratio
A1	5.8	.074	5.3	.069	0.9	.011	2.5	.033	5.5	.071	29.6	.380	12.4	.159	15.8	.203
C1	3.9	.051	3.8	.050	.8	.011	3.3	.044	1.8	.024	23.9	.312	27.4	.357	11.6	.151
C2	6.5	.076	7.3	.085	0.9	.010	2.0	.024	4.8	.056	41.1	.477	15.0	.174	8.6	.100
C3	5.8	.071	8.8	.108	0.7	.008	3.2	.039	2.4	.030	37.0	.454	15.5	.191	8.1	.099
C4	6.4	.062	8.7	.083	0.7	.007	4.0	.039	3.9	.037	42.8	.413	25.2	.243	12.1	.116
E1	5.5	.066	4.0	.048	0.5	.006	2.7	.032	6.0	.072	37.0	.446	8.7	.105	18.6	.224
M1	14.2	.172	5.4	.065	0.4	.005	1.8	.022	4.2	.050	34.9	.423	13.0	.157	8.7	.105
M2	6.3	.084	4.2	.056	1.5	.020	1.6	.021	4.4	.058	33.0	.437	15.3	.203	9.2	.122
N1	13.7	.157	10.2	.117	0.6	.007	0.8	.010	4.8	.056	34.9	.401	13.2	.152	8.6	.099
P1	5.2	.062	9.8	.116	0.9	.011	1.3	.016	4.3	.050	29.6	.350	12.2	.144	21.2	.251
S1	13.6	.128	7.7	.072	0.5	.005	3.1	.029	2.6	.025	43.6	.412	23.5	.222	11.4	.107
S2	5.3	.064	5.9	.071	1.0	.012	2.7	.033	4.5	.055	27.9	.336	18.0	.217	17.6	.212
S3	6.9	.064	5.7	.053	0.6	.006	5.9	.055	2.7	.026	42.6	.397	26.4	.246	16.4	.153
V1	6.7	.066	7.0	.069	2.7	.027	3.3	.032	5.4	.053	50.3	.492	18.3	.179	8.5	.083
Average	7.6	.082	6.7	.076	0.9	.010	2.7	.026	4.1	.040	36.3	.409	17.4	.196	12.6	.145
Std Dev	3.4	.042	2.1	.022	0.6	.006	1.2	.016	1.2	.020	7.0	.050	5.7	.059	4.3	.053

TABLE 4

## Description of Heat Sources to Basement

House	Window Design			# Ducts	Air Circulation		Solar Gains (Direction)	Electrical Gains
	Direction	Area (m <sup>2</sup> )	Glazings		Summer	Furnace Circulation		
M1	N	.48	4	5	High	Normal	Negligible (N)	Low
E1		0		4				
S1	S	3.4	5	5*	Normal	Normal	Substantial	High
	N	2.34	3					
C1	S	7.2	2 <sup>+</sup> shutter	HW Heat				
C2	W	.24		3	Normal	Normal	Negligible (NE)	Avg
	N	.24						
A1		0		4.1 Return	Normal	Normal	None	Avg
V1	E	.6		6	Normal	Normal	Negligible (E)	Avg
P1	N	.42		2				
	E	.42		4				
C3	S	2.51		2				
	S	2.22		3				
S2	S	3.08		4	Normal	Normal	Negligible (N)	Low
	N	.24		1				
C4	E	1.2		4*				
	S	1.1		2*				
N1	S	3.6		4	Low	Low	None	Low
				2				
S3	S	5		6	Normal	High	Negligible (Covered)	Low
M2	E	.9		4*	Low	Low	Small	High
		.8	3					

\* Estimated

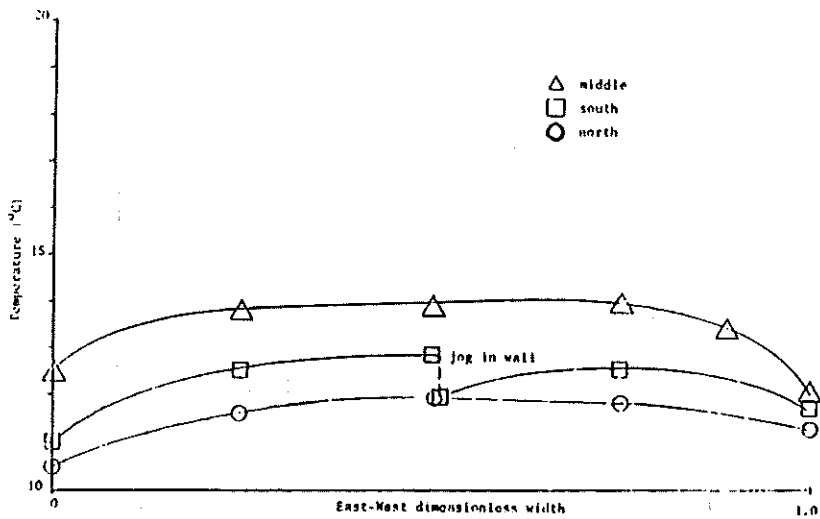


Figure 1. Floor temperature profiles for house A1, May 1981, air temperature  $14.8^{\circ}\text{C}$  @ .8 m height, slab floor, house unoccupied

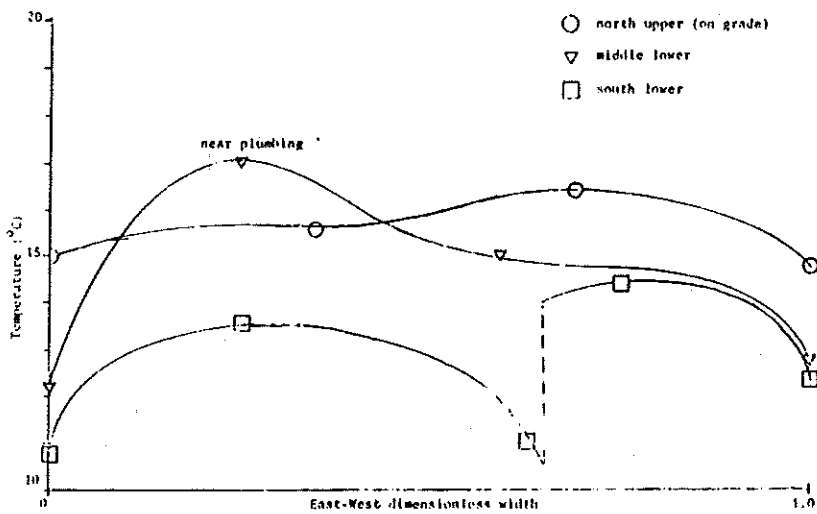


Figure 2. Floor temperature profiles for house P1, May 1981, air temperature  $17.3^{\circ}\text{C}$  @ .8 m height, slab floor

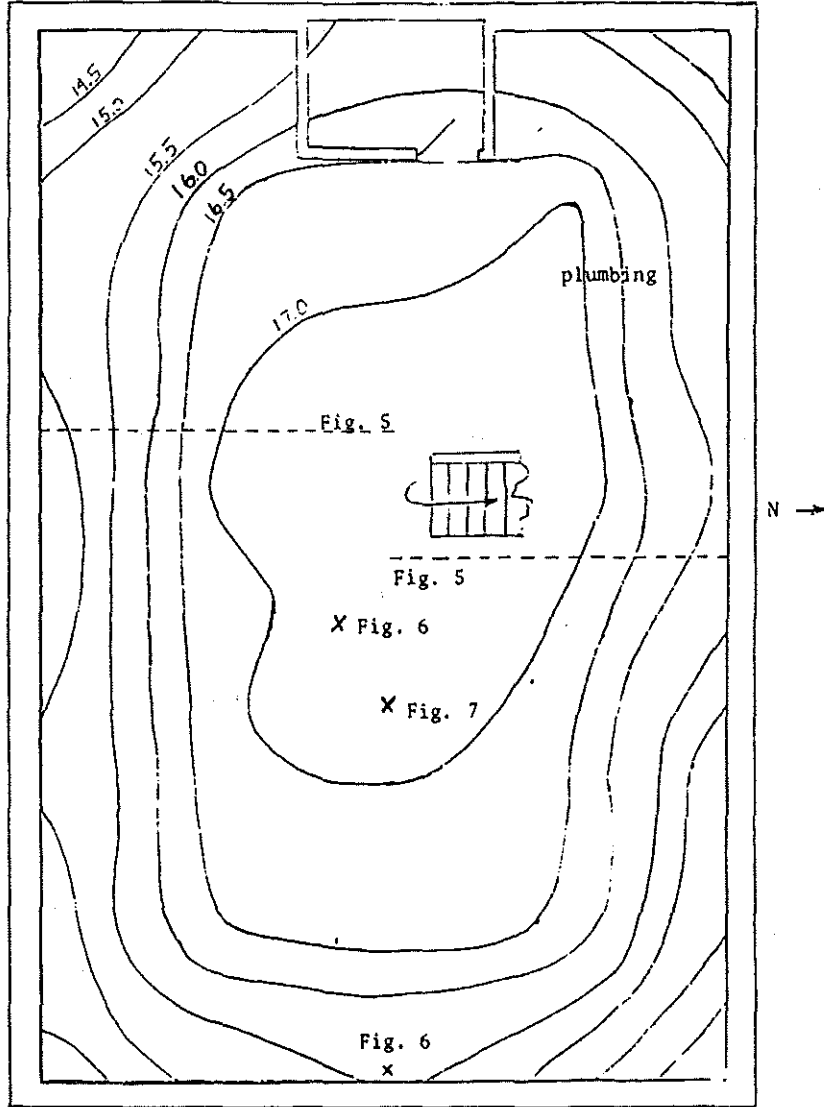


Figure 3. Floor temperature contours °C for house M1, June 10, 1981, house unoccupied

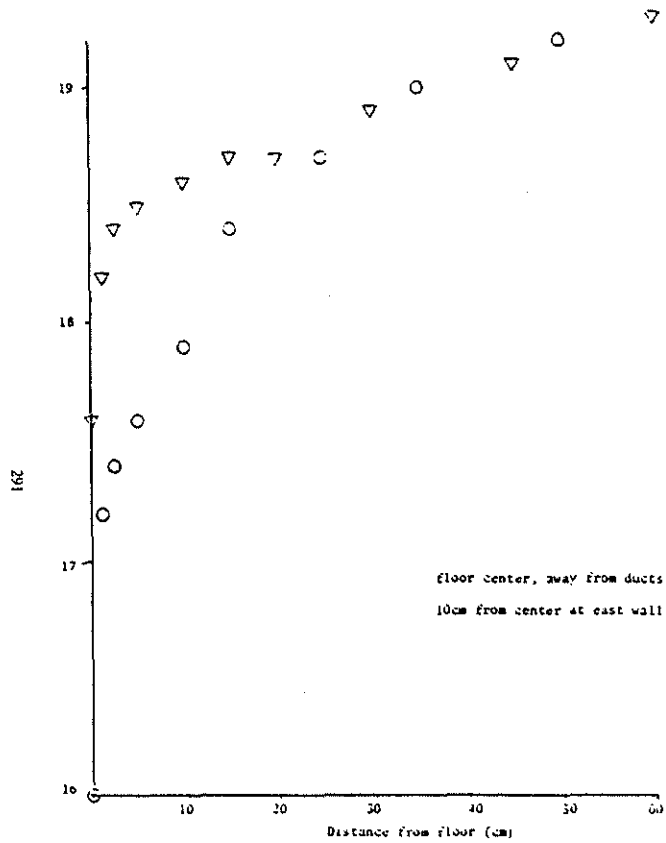


Figure 4. Air temperature profiles, house M1

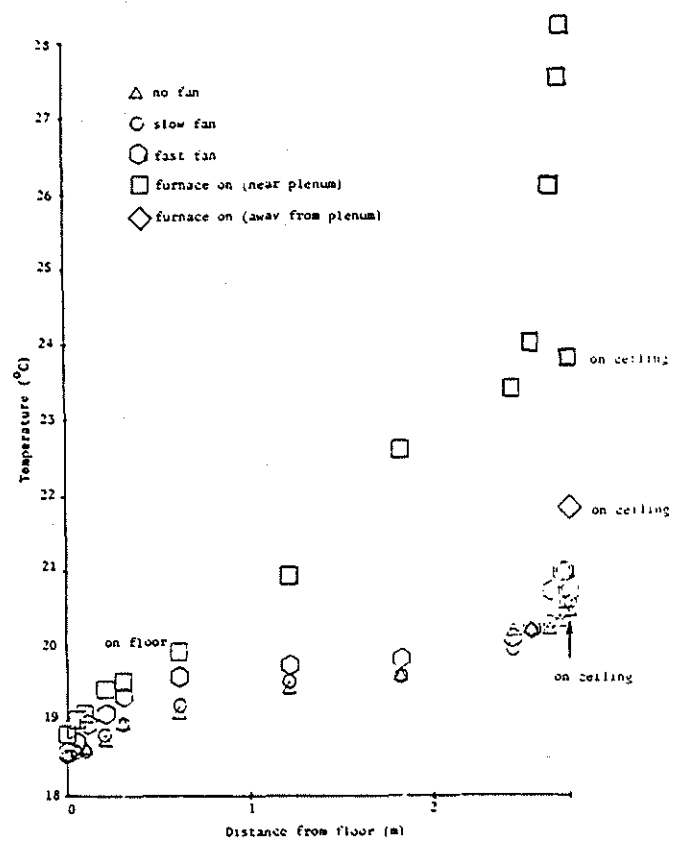


Figure 5. Air temperature profiles for house M1, June 23, 1981

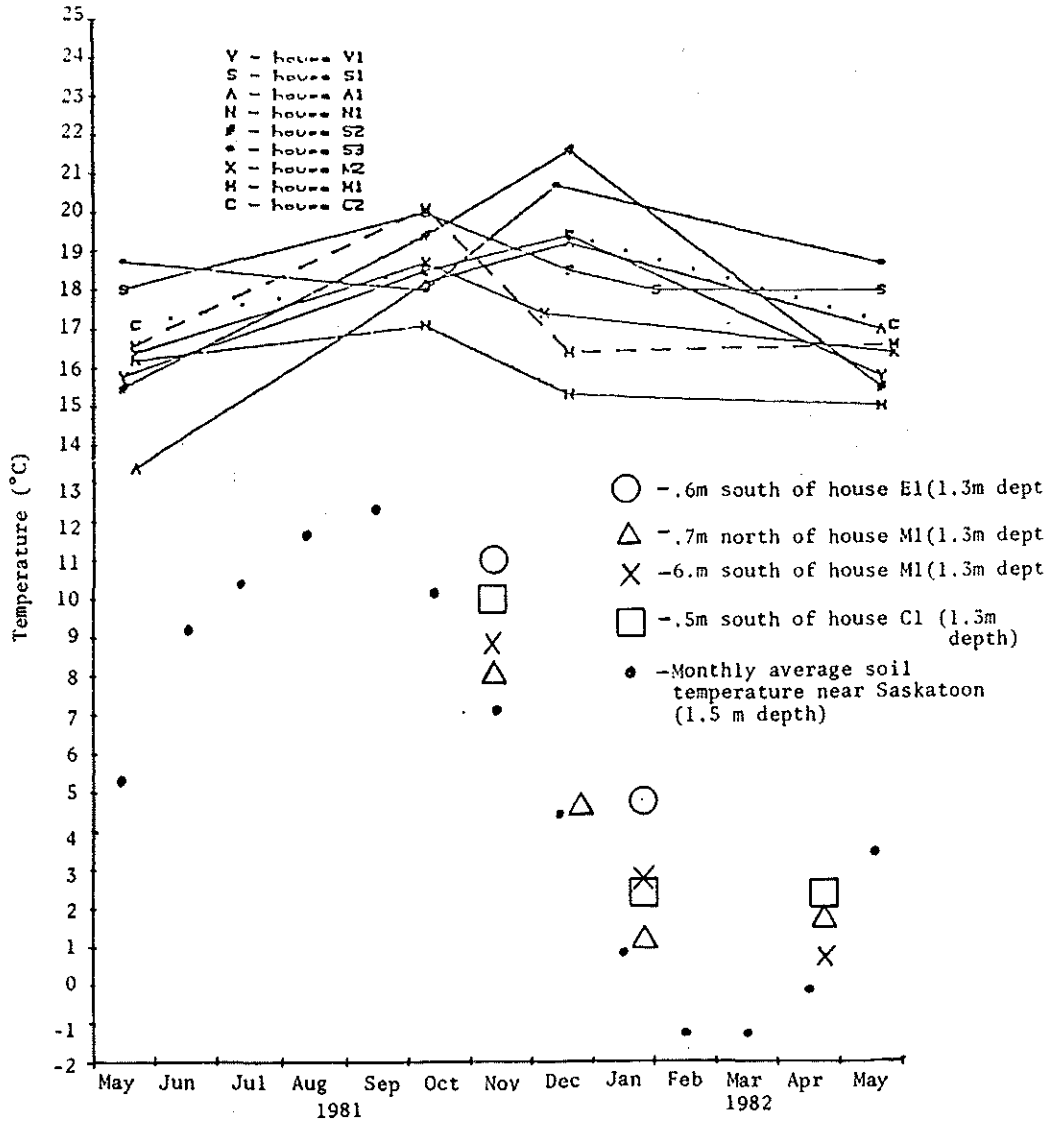


Figure 6. Measured floor and soil temperatures



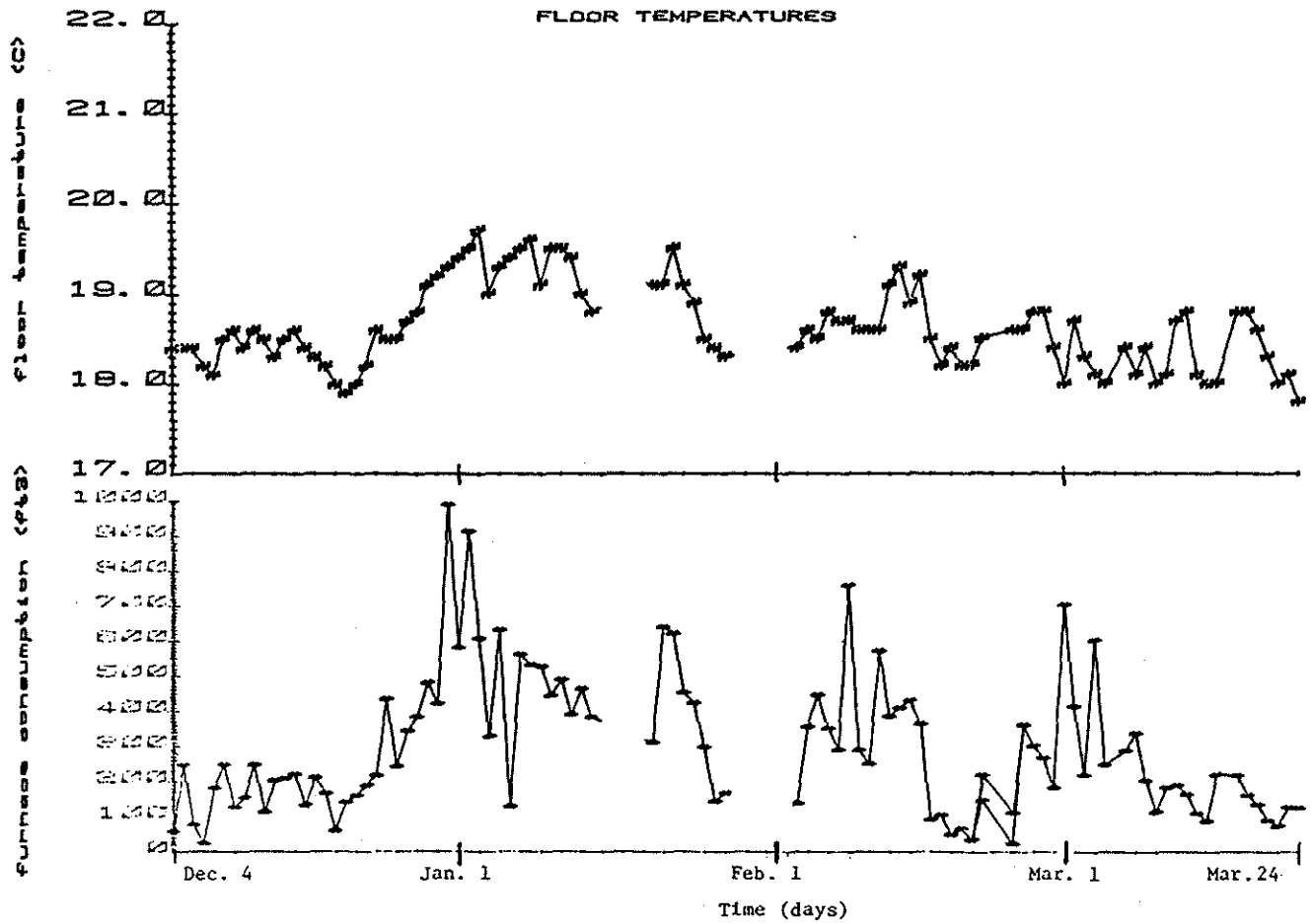


Figure 7. Measured basement floor temperature and furnace natural gas consumption Dec. 4, 1981 to March 24, 1982

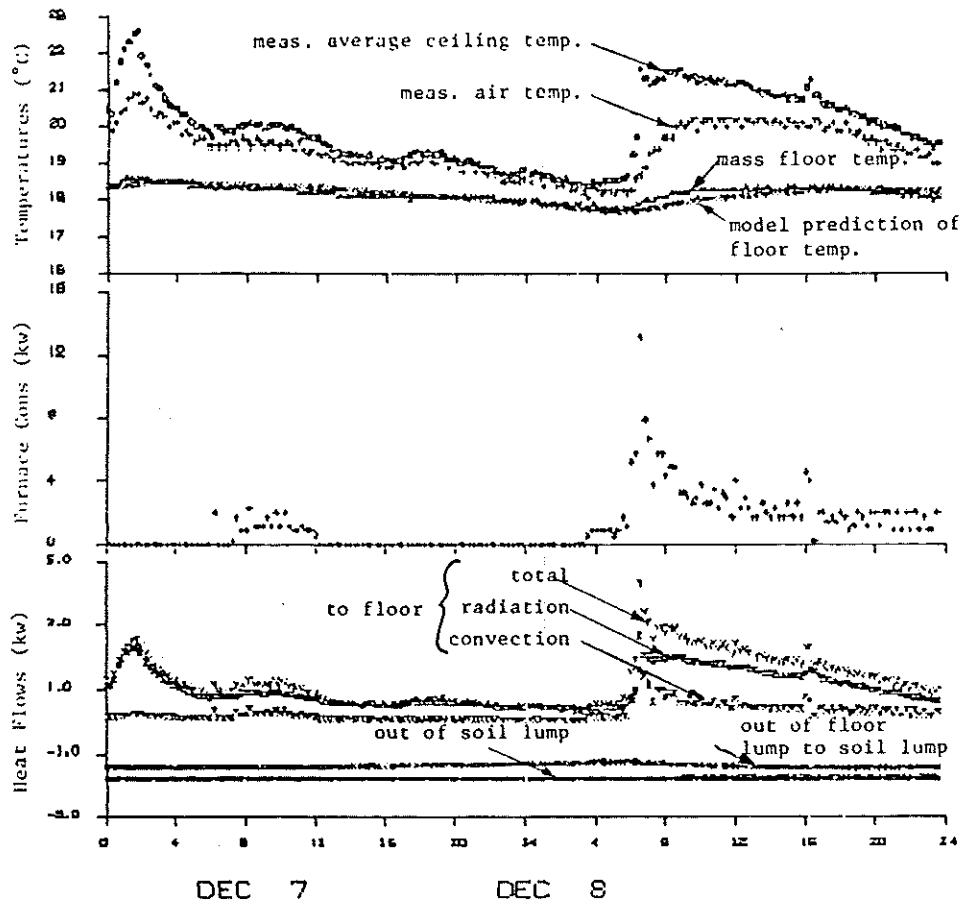


Figure 8. Measured and predicted basement floor temperatures and heat rates

## Discussion

D.T. Grimsrud, Lawrence Berkeley Lab., Univ. of California, Berkeley: What was the percentage loss in the average house due to infiltration? What was the nominal ventilation rate with the heat exchangers in place? Was there evidence of air quality problems in the houses?

R.W. Besant: The percentage loss due to infiltration, including forced air circulation through the air-to-air heat exchangers, was calculated using data from house pressure air infiltration tests at 50 pa and from air-to-air heat exchangers flow rate and performance. Using this information, the average percentage loss due to air infiltration was calculated to be 14.5%.

The nominal ventilation rates through the heat exchangers were measured on several occasions using hot wire anemometer velocity profiles in connecting ducts with the heat exchangers under normal operation. At first it was observed that there were a number of faults in the installation and operation of the air-to-air heat exchangers. After these were corrected as far as practical, it was observed that the average air change rate in the houses due to airflow through the air-to-air heat exchanger was 20 L/s. The maximum value was 49 L/s whereas the minimum value for flow through the air-to-air heat exchanger was not measured accurately due to cross flow within the heat exchanger itself. In this latter case, the air ventilation provided by the air-to-air heat exchanger was insufficient to avoid excess humidity and air quality problems in the houses.

Grimsrud: Did the heat exchangers experience freezing problems?

Besant: Most of the heat exchangers were designed to have a defrost cycle included in their operation. Where these defrost cycles were used, there was no problem with frosting; where they were not, there were some problems which resulted in poor quality air inside the houses.

R.R. Jones, National Bureau of Standards, Washington, DC: Can you describe the air distribution system for the subject houses, especially with regard to how the basement slab was impacted?

Besant: All the houses except one had a forced air circulation system that was activated by the furnace. The one without an active air circulation system was heated by a baseboard hot water system and the wooden floor was mounted on 10 cm sleepers without insulation. The others were all uninsulated concrete. Heat was supplied to these basements by ceiling ventilation ducts and vents. When the furnace fan was on, the air was jetted down toward the basement floor through the number of ducts outlined in Tab. 4 of the paper.

R. Crenshaw, Lawrence Berkeley Lab., Univ. of California, Berkeley: Why did you locate the vapor barrier inside the wall?

Besant: Maintaining airtight vapor barriers in low energy houses has been a major problem during the construction of houses. The problem has been resolved to some extent by incorporating the vapor barrier into the framing stage, specifying higher quality vapor barriers (150 m high quality polyethylene), caulking the vapor barrier only between clamped solid surfaces using nonhardening caulking compounds and avoidance of damage by other tradesmen such as plumbers, electricians, and drywallers. This last step involved placing the vapor barrier far enough inside the insulated wall system so that plumbers, electricians, and drywallers had no need to penetrate the vapor barrier under normal conditions of indoor air temperature and relative humidity and outdoor air temperatures.

Crenshaw: What was the depth of the frost line, and what was the average ground temperature at eight inches?

Besant: The frost line was not measured at each house, rather a number of ground temperatures were taken at the 1.3 m depth, including one taken at 1.5 m in undisturbed soil far from the houses. The results in Fig. 6 showed that there was no frost in any of the locations at the time of these tests except in the undisturbed soil region at 1.5 m in February and March.

The long-term average frost penetration depth in undisturbed soil in this location is 1.7 m, which occurs at the end of March. Average soil temperatures at 8 in. (10 cm) were not measured, but the average temperature at 10 cm in undisturbed soil in this region is about 3°C.

Crenshaw: Where did you place the footing to avoid heaving?

Besant: To avoid frost heaving of foundation footings, most houses had rigid styrofoam placed horizontally above the footings adjacent to the wall and protruding 2 ft (.67 m) out from the wall. The fact that the basement floors were uninsulated would also help to prevent frost under the footings.